A Linear Metal-Metal Bonded Tri-Iron Single-Molecule Magnet

Anandi Srinivasan, Rebecca Musgrave, Mathieu Rouzières, Rodolphe Clérac, John Mcgrady, Elizabeth Hillard

A Linear Metal-Metal Bonded Tri-Iron Single-Molecule Magnet

Anandi Srinivasan,[a] Rebecca A. Musgrave,[a] Mathieu Rouzières,[a] Rodolphe Clérac,*[a] John E. McGrady,[b] Elizabeth A. Hillard*[a]

Univ. Bordeaux, CNRS, Centre de Recherche Paul Pascal, UMR 5031, F-33600, Pessac, France, E-mail: elizabeth.hillard@icmcb.cnrs.fr & clerac@crpp-bordeaux.cnrs.fr
Department of Chemistry, University of Oxford, South Parks Road, Oxford, OX1 3QZ, United Kingdom

Abstract: The linear trinuclear complex cation $[Fe_3(DpyF)_4]^{2+}$ was prepared as $[Fe_3(DpyF)_4](BF_4)_2{\cdot}2CH_3CN$. With large Fe–Fe distances of 2.78 Å, this complex demonstrates intramolecular ferromagnetic coupling between the anisotropic Fe^{II} centers (J/k_B = +20.9(5) K) giving an S_T = 6 ground state and exhibits single-molecule magnet properties.

The pursuit of molecule-based magnetic storage units has inspired enormous scientific activity, with a key challenge being the conception of new single-molecule magnets (SMMs) working at liquid nitrogen temperatures or above.[1] One approach has been to increase the thermal energy barrier of the Orbach-like relaxation by maximizing the ground spin state. Although very high spin polynuclear complexes can be obtained,[2] negligible magnetic anisotropy often results in a poorly isolated ground state. To overcome this, one strategy is to increase the intramolecular magnetic coupling using, for example, radical-based spin mediators to promote the parallel alignment of the metal spins (i.e. an effective ferromagnetic coupling which is independent of the nature of the magnetic interaction between the bridging radical and metal centers).[3]

Ferromagnetic coupling (FM) can also be observed in direct metal-metal interactions, particularly for valence-delocalized iron clusters,[‡] which often exhibit maximal ground spin states.[4] The simplest examples include di-iron paddlewheel complexes, such as an Fe^{I}-Fe^{I} complex with an intermetallic distance of 2.127 Å (S_T = 3),[5] mixed-valent Fe^{II}-Fe^{I} complexes[6] with distances of *ca*. 2.2 Å (S_T = 7/2), and two Fe^{II}-Fe^{II} complexes with distances of 2.287 and 2.462 Å (S_T = 4).[7] The face-sharing bioctahedral S_T = 9/2 complex $[(Me_3tacn)_2Fe_2(\mu^2\text{-}OH)_3]^{2+}$, has yet a longer Fe−Fe distance of 2.510 Å.[8] Eventually, the Fe-Fe distance becomes too large to mediate spin coupling; as in $Fe_2(\mu\text{-}DPhBz)_2(\eta^2\text{-}DPhBz)_2$ (d_{Fe-Fe} = 3.124 Å), with a magnetic moment compatible with non-interacting S_{Fe} = 2 centres.[7a]

Clusters with three iron ions can adopt a triangular or, more rarely, a linear arrangement of atoms. Examples of high-spin triangular complexes include the mixed-valent S_T = 11/2 Fe_3 (and related S_T = 19/2 Fe_6) clusters, with Fe–Fe distances ranging from *ca.* 2.4 to 2.7 Å.[9] Maximal spin states have also been predicted for linear iron clusters,[10] although only four such compounds have been reported. Recently, a trinuclear compound with three bridging 2,6-bis[(trimethylsilyl)amido]pyridine ligands was obtained with FM coupling between the Fe^{II} centers (2.442 Å).[11] Additionally, the tetranuclear complexes $Fe_4(tpda)_3Cl_2$[12] and $Fe_4(tpda)_3Br_2$,[13] with mixed bridging-chelating tripyridyldiamido modes and long Fe–Fe distances of > 2.9 Å, were modelled as consisting of two FM coupled Fe_2 pairs, with antiferro-

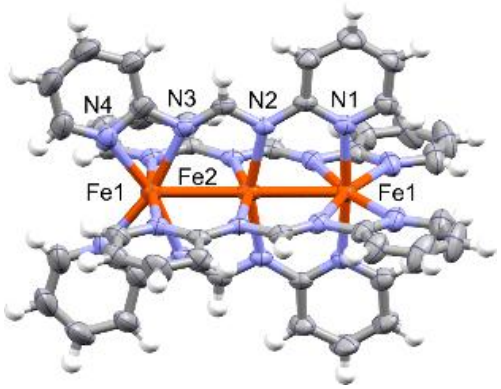

Figure 1. Thermal ellipsoid (50%) diagram of the cation in **1** at 270 K from single crystal X-ray diffraction data.

magnetic (AF) inter-pair interactions. In 1998, a tri-iron cluster with a similar mixed coordination mode, $[Fe_3(DpyF)_4](PF_6)_2$, (DpyF = dipyridylformamide), was reported to have a room-temperature χT value of 16 cm^3 K mol^{-1}, much higher than that expected for three isolated Fe^{II} centers, once again suggesting FM coupling between the Fe^{II} spins.[14]

Motivated by our interest in the magnetic properties of linear clusters,[15] we have prepared the BF_4^- analogue $[Fe_3(DpyF)_4](BF_4)_2$ to study its static and dynamic magnetic properties. $[Fe_3(DpyF)_4](BF_4)_2{\cdot}2CH_3CN$ (**1**, Figure 1) was synthesized using an adaptation of the literature protocol,[14] by refluxing LiDpyF, $FeCl_2$ and $TlBF_4$ in THF and recrystallizing the ensuing pale yellow precipitate from the diffusion of diethyl ether into an acetonitrile solution (ESI). It crystallizes in the space group *I*4/*m* (Table S1) such that the four fold axis is co-linear with the metal axis and the central Fe^{II} ion is bisected by a glide plane perpendicular to the metal axis, giving one unique Fe(1)–Fe(2) distance of 2.7838(5) and 2.7742(6) Å at 270 and 100 K, respectively. The cation displays distorted octahedral terminal Fe^{II} sites and a tetrahedrally distorted square planar central Fe^{II} ion (Table S3). The terminal Fe(1)–N distances average 2.191[2] Å for both temperatures, while the central Fe(2)–N(2) distance is 2.1436(18) and 2.1431(18) Å (Table S2), consistent with HS Fe^{II} centres and similar to those reported for $[Fe_3(DpyF)_4](PF_6)_2$.[14] One of the BF_4^- anions and the solvent molecules could not be modelled atomistically; solvent masking in Olex 2[16] suggested the presence of two acetonitrile molecules per formula unit.

The static magnetic susceptibility, χ, was measured on a polycrystalline sample of **1** mixed with mineral oil (Figure 2). The χT value at 300 K is 15.3 cm^3 K mol^{-1}, significantly higher than the sum of Curie constants for three uncoupled high-spin Fe^{II} centers (9.0 cm^3 K mol^{-1} for g = 2). Upon decreasing the temperature, the χT value increases continuously, reaching a maximum value of 25.8 cm^3 K mol^{-1} at 22 K, revealing dominant FM coupling between the three Fe^{II} S = 2 spins. The maximum value is higher than that expected from an S_T = 6 system (21.0 cm^3 K mol^{-1}, g = 2), suggesting the contributions from orbital momentum, leading to a g factor higher than 2 (as expected for high-spin octahedral Fe^{II} centers). Below 20 K, the χT value at low field (0.1 T) decreases slightly to reach a minimum value of 21.7 cm^3 K mol^{-1} at 1.85 K, likely due to magnetic anisotropy

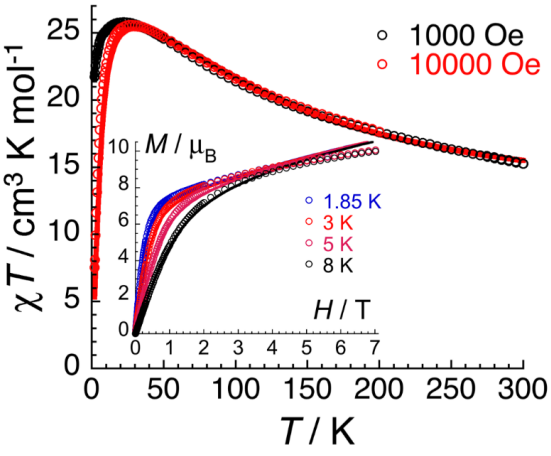

Figure 2. Temperature dependence of the χT product (where χ is the molar magnetic susceptibility (M/H) per complex and T the temperature) in an applied dc magnetic field of 0.1 and 1 T for **1**. Inset: Field dependence of the magnetization for **1** below 8 K. Solid lines are the best fits to the model described in the text.

and/or AF interactions between cation moments. Variable field magnetization data below 8 K (Figure 2, inset and Figure S1), do not saturate even at 7 T, reaching a maximum value of 10.7 $\mu_{B,}$ lower than the 12 μ_B expected for an S_T = 6 species. This high field feature, and the non-superposition of the $M = f(HT^{-1})$ curves (Figure S1), strongly suggest the presence of a significant magnetic anisotropy. In the literature, magnetic data for linear iron clusters have been treated either using an exchange-coupled model, when FM exchange is weak ($|J/k_B|$<50 K)[7b,12] or a delocalized macrospin model in the strong coupling limit ($|J/k_B|$>300 K).[9a,9c] In the present case, a simple macrospin model would not capture the temperature dependence of the χT product (Figure 2), and therefore the experimental data were fitted numerically (PHI[17]) considering the following anisotropic Heisenberg Hamiltonian:

$$\hat{H} = -2J\left(\hat{S}_{\mathrm{Fe}-1}\cdot\hat{S}_{\mathrm{Fe}-2} + \hat{S}_{\mathrm{Fe}-2}\cdot\hat{S}_{\mathrm{Fe}-3}\right) + 3D_{\mathrm{Fe}}\hat{S}^2_{\mathrm{Fe},z}$$

where J denotes the intramolecular interaction between Fe^{II} spins, $\hat{S}_{\mathrm{Fe}-\mathrm{i}}$ is the spin operator for each metal ion centre (S_{Fe} = 2) and D is the axial ZFS parameter. The best fit parameters, J/k_B = +20.9(3) K, D/k_B = –6.2(2) K and g = 2.23(5), reproduce well the experimental data shown in Figures 2 and S1. Notably, the fit was not significantly improved by incorporating a rhombic ZFS parameter or intermolecular interactions in the model and degraded strongly upon forcing D to be positive. The estimated FM interaction in $[Fe_3(DpyF)_4](BF_4)_2{\cdot}2CH_3CN$ (J/k_B = +20.9 K) is slightly larger than in $Fe_4(tpda)_3X_2$ (J/k_B = +10.1 to +15.4 K),[12,13] which possess longer Fe–Fe distances (> 2.9 Å vs. 2.78 Å).

Further insight into the ground state electronic structure on the cation in **1** was obtained using density functional theory (DFT) as implemented in ORCA v.4.2.1,[18] using X-ray coordinates adjusted to D_{2d} symmetry without further optimization. The performance of DFT in describing exchange coupling has been reviewed extensively,[19] and the choice of functional has a substantial impact, particularly in cases where the ground state involves FM exchange. Following recommendations from Illas et al.,[20] we discuss here results obtained with the hybrid B3LYP functional,[21] and the sensitivity of the results to other choices is discussed in ESI. We have identified a number of different FM configurations with S_T = 6, along with a broken-symmetry (AF) state which is an approximate quintet with M_S = 2. The lowest-energy configuration does indeed prove to be FM ($^{13}B_2$, S_T = 6): The Fe^{II} manifold of Kohn-Sham orbitals is shown in Figure 3, with only the □-manifold shown here for simplicity. The orbital array shows the 15 metal-based orbitals split into a lower band of 10 that are approximately Fe–N non-bonding and a higher band of 5 that are Fe–N antibonding. The very different local coordination environments of the terminal and inner Fe^{II} ions (octahedral and distorted square-planar, respectively), lead to different high-spin electronic configurations: for the two terminal Fe^{II} ions, the 6th (spin-β) 3*d* electron occupies a d_{z^2} orbital ($1a_1$ and $1b_2$ in Figure 3), while for the inner Fe^{II} ion, the 6th electron occupies a d_{xy} orbital ($1b_1$), with Fe-Fe δ character. The σ manifold therefore makes a FM contribution to exchange coupling through a spin delocalization/double exchange mechanism (see inset in Figure 3), while the δ manifold makes an AF superexchange contribution according to the Goodenough-Kanamori rules, albeit a weak one due to the limited δ overlap. The sum of the two components, FM coupling in the σ manifold and weak AF coupling in δ, gives rise to the FM alignment observed in the magnetic measurements.

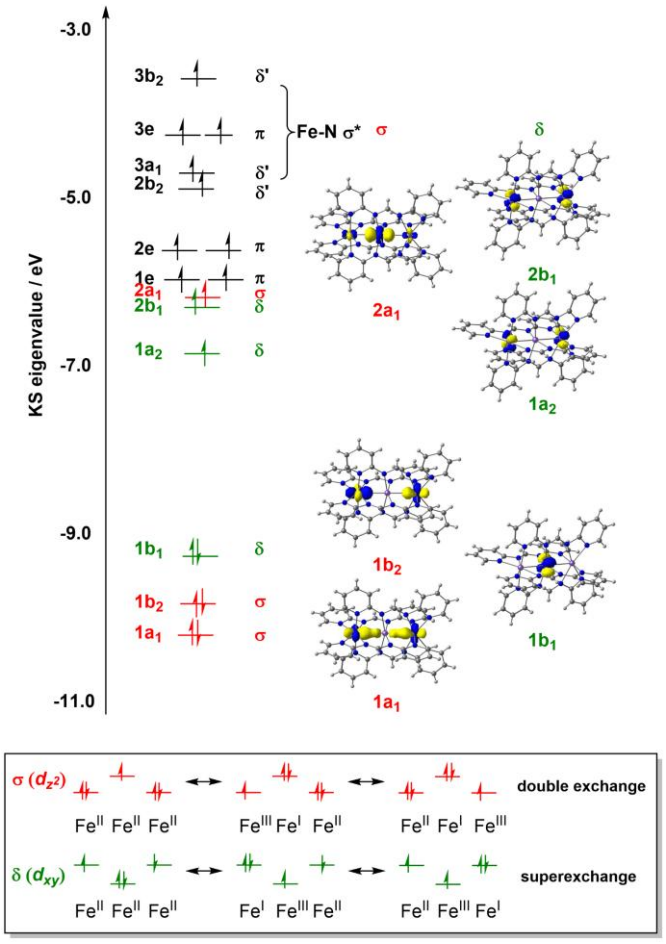

Figure 3. Kohn-Sham orbital energy diagram for the $^{13}B_2$ ground state of $[Fe_3(DpyF)_4]^{2+}$. Interactions with σ, π, δ and δ′ symmetry are mediated by d_{z^2}, $d_{xz/yz}$, d_{xy} and $d_{x^2-y^2}$ orbitals, respectively. Eigenvalues and eigenfunctions shown are for the spin-β manifold. Isosurfaces are shown only for the orbitals of σ and δ symmetry that are involved in Fe-Fe exchange coupling. The schematic configurations shown in the inset illustrates the FM and AF contributions of double- and superexchange in the σ and δ manifolds, respectively.

The electronic structure can be mapped onto the Heisenberg ladder using a broken-symmetry state with M_S = 2, where the spin moment on the central Fe ion is inverted relative to the FM ground state. While the near orbital degeneracy of the Fe^{II} ion complicates the mapping of spin-state energies onto a simple Heisenberg-type Hamiltonian,[22] we can use the computed energies of the S_T = 6 and M_S = 2 states to extract an estimate of the exchange coupling constant, J/k_B = +43.2 K (ESI). While this number is higher than the experimental value of +20.9 K, it is within the normal range of accuracy shown by DFT in the FM regime.

The dominance of FM coupling, the detection of magnetic anisotropy and a negative D value led us to investigate potential SMM properties. In the absence of an external dc-field, no frequency dependence in either the in-phase (χ') or out-of-phase (χ'') component of the ac susceptibility was observed above 1.8 K with ac frequencies up to 10 kHz (ESI). The application of an external dc-field led to appearance of frequency and temperature dependent ac signals (Figures 4 and S2, ESI), revealing the slow dynamics of the magnetization and consequently, its SMM properties. The χ' vs. ν and χ'' vs. ν data at 1.9 K in different dc-fields (Figure S2, ESI) and at different temperatures under 0.2 T (Figure 4) were fit to the generalized Debye model[23] to obtain the field and temperature dependence of the magnetization relaxation time (τ) characteristic of this S_T = 6 SMM (Figure S5). To analyse the paramagnetic relaxation, four mechanisms are usually invoked: quantum tunneling of the magnetization (QTM),[24,25] Orbach-type (i.e., thermally activated, Arrhenius behavior),[25-27] Raman[27] and direct[28] processes. The paramagnetic relaxation rate (τ^{-1}) can be then decomposed in four terms:

$$\tau^{-1} = \tau_{Raman}^{-1} + \tau_{Direct}^{-1} + \tau_{Arrhenius}^{-1} + \tau_{QTM}^{-1}$$

possessing their own thermal and dc-field dependences with a collection of eight independent parameters:

$$\tau^{-1} = C\frac{1+C_1H^2}{1+C_2H^2}T^n + ATH^m + \tau_0^{-1}\exp\left(-\frac{\Delta}{k_BT}\right) + \frac{B_1}{1+B_2H^2}$$

Considering that the magnetization relaxation is observed in a small experimental window (0.02-1 T, 1.8-3 K, 0.115-10 kHz; Figure S5), it is unreasonable to try to extract accurately the whole set of parameters. Nevertheless, a few hypotheses can be formulated by a simple analysis of the relaxation time. At low dc-field (Figure S5a), the characteristic frequency decreases from 10 kHz at 0.02 T down to 140 Hz at 0.3 T suggesting the presence of QTM relaxation, even if a Raman process cannot be completely excluded with $C_2 > C_1$. Above 0.3 T, the relaxation time is only weakly field dependent, in disagreement with direct (in H^{-4} or H^{-2}) or Raman (in H^{-2} with $C_2 << C_1$) mechanisms. Therefore, the paramagnetic relaxation in **1** seems to be dominated by Orbach-type and QTM pathways. Between 1.8 and 3 K, the ln(τ) vs. T^{-1} plot (Figure S5b) is linear and thus compatible with a thermally activated relaxation with a pre-exponential factor, τ_0, of 9(1) × 10^{-9} s and an energy gap, Δ_{eff}/k_B, of 22(1) K. Nevertheless, this value is ten times lower than that expected ($\Delta/k_B = DS_T^2/k_B$ = 223 K) from the estimated magnetic anisotropy (D/k_B = –6.2 K) and the spin-ground state (S_T = 6) suggesting that our experimental window may cover a crossover regime between these two relaxation pathways.

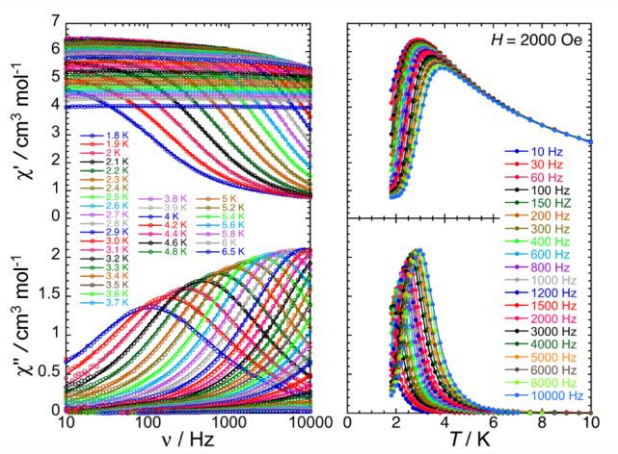

Figure 4. ac frequency (left) and temperature (right) dependence of the real (χ', top) and imaginary (χ'', bottom) parts of the ac susceptibility for **1** at 0.2 T, for ac frequencies of 10-10000 Hz and 1.8-10 K. Solid lines on the χ' and χ'' vs. ν plots are generalised Debye fits[23] of the ac data used to extract the temperature dependence of the relaxation time (Figure S5) as well as α, ν, χ_0', χ_∞' and χ_0'-χ_∞' (Fig. S4.)

In conclusion, $[Fe_3(DpyF)_4](BF_4)_2 \cdot 2CH_3CN$ contains a rare example of a linearly-disposed trinuclear cluster cation, with ferromagnetically coupled Fe^{II} ions and an S_T = 6 ground state, consisting of singly-occupied nearly degenerate metal-based molecular orbitals. The Fe–Fe distance (2.8 Å) is amongst the longest observed to mediate FM coupling. The magnetic data was modeled with an anisotropic Heisenberg Hamiltonian, giving J/k_B = +20.9(3) K and D/k_B = –6.2(2) K. The combination of the strong magnetic anisotropy and the energetically well-separated ground state likely yield the SMM properties, which appear to involve QTM and Orbach-like relaxations.

Electronic Supplementary Information (ESI) available: Synthesis, crystallography, Shape analysis, magnetic measurements and theoretical calculations. See DOI: 10.1039/D1CC05043E. Structures of **1** at 270 and 100 K can be found in the Cambridge Structural Database CCDC 2025912-2025913.

Conflicts of interest

There are no conflicts to declare.

Acknowledgements

This work was supported by the CNRS, the French Ministry for Higher Education, Research and Innovation, the Regional Council of Nouvelle Aquitaine, the University of Bordeaux, Quantum Matter Bordeaux and the EU Horizon 2020 Research and Innovation Programme under grant agreement No. 752684. We thank S. Exiga and V. Bulicanu for technical assistance.

Notes and references

1 (a) C. A. P. Goodwin, F. Ortu, D. Reta, N. F. Chilton and D. P. Mills, *Nature*, 2017, **548**, 439. (b) F.-S. Guo, B. M. Day, Y.-C. Chen, M.-L. Tong, A. Mansikkamäki and R. A. Layfield, *Angew. Chem. Int. Ed.*, 2017, **56**, 11445. (c) F.-S. Guo, B. M. Day, Y.-C. Chen, M.-L. Tong, A. Mansikkamäki and R. A. Layfield, *Science*, 2018, **362**, 1400.

2 (a) A. M. Ako, I. J. Hewitt, V. Mereacre, R. Clérac, W. Wernsdorfer, C. E. Anson and A. K. Powell, *Angew. Chem. Int. Ed.*, 2006, 118, 5048. (b) W.-P. Chen, J. Singleton, L. Qin, A. Camón, L. Engelhardt, F. Luis, R. E. P. Winpenny and Y.-Z. Zheng, *Nat. Commun.*, 2018, **9**, 2107. (c) M. Charalambous, E. E. Moushi, T. N. Nguyen, C. Papatriantafyllopoulou, V. Nastopoulos, G. Christou, A. J. Tasiopoulos, *Front. Chem.*, 2019, **7**, 96.

3 (a) I.-R. Jeon, J. G. Park, D. J. Xiao and T. D. Harris, *J. Am. Chem. Soc.*, 2013, **135**, 16845. (b) J. O. Moilanen, N. F. Chilton, B. M. Day, T. Pugh and R. A. Layfield, *Angew. Chem. Int. Ed.*, 2016, **55**, 5521. (c) J. Wang, J.-N. Li, S.-L. Zhang, X.-H. Zhao, D. Shao and X.-Y. Wang, *Chem. Commun.*, 2016, **52**, 5033. (d) M. A. Lemes, G. Brunet, A. Pialat, L. Ungur, I. Korobkov and M. Murugesu, *Chem. Commun.*, 2017, **53**, 8660. (e) S. Demir, M. I. Gonzalez, L. E. Darago, W. J. Evans and J. R. Long, *Nat Commun*, 2017, **8**, 2144. (f) B. S. Dolinar, D. I. Alexandropoulos, K. R. Vignesh, T. James and K. R. Dunbar, *J. Am. Chem. Soc.*, 2018, **140**, 908. (g) X. Ma, E. A. Suturina, M. Rouzières, M. Platunov, F. Wilhelm, A. Rogalev, R. Clérac and P. Dechambenoit, *J. Am. Chem. Soc.*, 2019, **141**, 7721.

4 (a) S. Kuppuswamy, T. M. Powers, B. M. Johnson, M. W. Bezpalko, C. K. Brozek, B. M. Foxman, L. A. Berben and C. M. Thomas, *Inorg. Chem.*, 2013, **52**, 4802. (b) S. K. Dutta, J. Ensling, R. Werner, U. Flörke, W. Haase, P. Gütlich and K. Nag, *Angew. Chem. Int. Ed.*, 1997, **36**, 152.

5 L. Fohlmeister, S. Liu, C. Schulten, B. Moubaraki, A. Stasch, J. D. Cashion, K. S. Murray, L. Gagliardi and C. Jones, *Angew. Chem. Int. Ed.*, 2012, **51**, 8294.

6 (a) C. M. Zall, D. Zherebetskyy, A. L. Dzubak, E. Bill, L. Gagliardi and C. C. Lu, *Inorg. Chem.*, 2012, **51**, 728. (b) F. A. Cotton, L. M. Daniels, L. R. Falvello, J. H. Matonic and C. A. Murillo, *Inorg. Chim. Acta*, 1997, **256**, 269. (c) F. A. Cotton, L. M. Daniels, L. R. Falvello and C. A. Murillo, *Inorg. Chim. Acta*, 1994, **219**, 7.

7 (a) F. A. Cotton, L. M. Daniels, J. H. Matonic and C. A. Murillo, *Inorg. Chim. Acta*, 1997, **256**, 277. (b) S. J. Tereniak, R. K. Carlson, L. J. Clouston, V. G. Young, E. Bill, R. Maurice, Y.-S. Chen, H. J. Kim, L. Gagliardi and C. C. Lu, *J. Am. Chem. Soc.*, 2014, **136**, 1842.

8 (a) S. Drüeke, P. Chaudhuri, K. Pohl, K. Wieghardt, X.-Q. Ding, E. Bill, A. Sawaryn, A. X. Trautwein, H. Winkler and S. J. Gurman, *J. Chem. Soc., Chem. Commun.*, 1989, 59. (b) X. Ding, E. L. Bominaar, E. Bill, H. Winkler, A. X. Trautwein, S. Drüeke, P. Chaudhuri and K. Wieghardt, *J. Chem. Phys.*, 1990, **92**, 178. (c) D. R. Gamelin, E. L. Bominaar, M. L. Kirk, K. Wieghardt and E. I. Solomon, *J. Am. Chem. Soc.*, 1996, **118**, 8085.

9 (a) R. Hernández Sánchez and T. A. Betley, *J. Am. Chem. Soc.*, 2015, **137**, 13949. (b) R. Hernández Sánchez, A. K. Bartholomew, T. M. Powers, G. Ménard and T. A. Betley, *J. Am. Chem. Soc.*, 2016, **138**, 2235. (c) R. H. Sánchez and T. A. Betley, *J. Am. Chem. Soc.*, 2018, **140**, 16792.

10 P. Szarek, W. Wegner and W. Grochala, *J. Mol. Model.*, 2016, **22**, 63.

11 G. L. Guillet, K. Y. Arpin, A. M. Boltin, J. B. Gordon, J. A. Rave and P. C. Hillesheim, *Inorg. Chem.*, 2020, **59**, 11238.

12 A. Nicolini, R. Galavotti, A.-L. Barra, M. Borsari, M. Caleffi, G. Luo, G. Novitchi, K. Park, A. Ranieri, L. Rigamonti, F. Roncaglia, C. Train and A. Cornia, *Inorg. Chem.*, 2018, **57**, 5438.

13 A. Nicolini, M. Affronte, D. J. SantaLucia, M. Borsari, B. Cahier, M. Caleffi, A. Ranieri, J. F. Berry and A. Cornia, *Dalton Trans.*, 2021, **50**, 7571.

14 F. A. Cotton, C. A. Murillo and X. Wang, *Inorg. Chem. Comm.*, 1998, **1**, 281.

15 (a) A. Cornia, L. Rigamonti, S. Boccedi, R. Clérac, M. Rouzières and L. Sorace, *Chem. Commun.*, 2014, **50**, 15191. (b) A. Srinivasan, X. Wang, R. Clérac, M. Rouzières, L. R. Falvello, J. E. McGrady and E. A. Hillard, *Dalton Trans.*, 2018, **47**, 16798. (c) A. Cornia, A.-L. Barra, V. Bulicanu, R. Clérac, M. Cortijo, E. A. Hillard, R. Galavotti, A. Lunghi, A. Nicolini, M. Rouzières, L. Sorace and F. Totti, *Inorg. Chem.*, 2020, **59**, 1763.

16 O. V. Dolomanov, L. J. Bourhis, R. J. Gildea, J. a. K. Howard and H. Puschmann, *J Appl Cryst*, 2009, **42**, 339.

17 N. F. Chilton, R. P. Anderson, L. D. Turner, A. Soncini and K. S. Murray, *J. Comput. Chem.*, 2013, **34**, 1164.

18 F. Neese, *WIREs Comput Mol Sci*, 2012, **2**, 73.

19 (a) G. David, N. Guihéry and N. Ferré, *J. Chem. Theory Comput.*, 2017, **13**, 6253. (b) P. Rivero, I. de P. R. Moreira, F. Illas and G. E. Scuseria, *J. Chem. Phys.*, 2008, **129**, 184110. (c) R. Valero, R. Costa, I. de P. R. Moreira, D. G. Truhlar and F. Illas, *J. Chem. Phys.*, 2008, **128**, 114103.

20 R. Costa, D. Reta, I. de P. R. Moreira and F. Illas, *J. Phys. Chem. A*, 2018, **122**, 3423.

21 P. J. Stephens, F. J. Devlin, C. F. Chabalowski and M. J. Frisch, *J. Phys. Chem.*, 1994, **98**, 11623.

22 A. Palii, B. Tsukerblat, S. Klokishner, K. R. Dunbar, J. M. Clemente-Juan and E. Coronado, *Chem. Soc. Rev.*, 2011, **40**, 3130.

23 K. S. Cole and R. H. Cole, *J. Chem. Phys.*, 1941, **9**, 341.

24 G. Christou, D. Gatteschi, D. N. Hendrickson, R. Sessoli, *MRS Bull.*, 2011, **25**, 66.

25 R. Sessoli, D. Gatteschi, A. Caneschi, M. A. Novak. *Nature*, 1993, **365**, 141.

26 D. Gatteschi, R. Sessoli, J. Villain, *Molecular Nanomagnets, Oxford University Press,* **2006**.

27 J. H. Van Vleck, *Phys. Rev.*, 1940, **57**, 426.

28 K. N. Shrivastava, *Phys. Stat. Sol. A*, 1983, **117**, 437.